

# Demonstration of a cavity coupler based on a resonant waveguide grating

Frank Brückner,<sup>1,\*</sup> Daniel Friedrich,<sup>2</sup> Tina Clausnitzer,<sup>1</sup> Oliver Burmeister,<sup>2</sup> Michael Britzger,<sup>2</sup> Ernst-Bernhard Kley,<sup>1</sup> Karsten Danzmann,<sup>2</sup> Andreas Tünnermann,<sup>1</sup> and Roman Schnabel,<sup>2</sup>

<sup>1</sup>*Institut für Angewandte Physik, Friedrich-Schiller-Universität Jena, Max-Wien-Platz 1, 07743 Jena, Germany*

<sup>2</sup>*Max-Planck-Institut für Gravitationsphysik (Albert-Einstein-Institut) and Institut für Gravitationsphysik, Leibniz Universität Hannover, Callinstrasse 38, 30167 Hannover, Germany*

[frank.brueckner@uni-jena.de](mailto:frank.brueckner@uni-jena.de)

**Abstract:** Thermal noise in multilayer optical coatings may not only limit the sensitivity of future gravitational wave detectors in their most sensitive frequency band but is also a major impediment for experiments that aim to reach the standard quantum limit or to cool mechanical systems to their quantum ground state. Here, we present the experimental realization and characterization of a cavity coupler, which is based on a surface relief guided-mode resonant grating. Since the required thickness of the dielectric coating is dramatically decreased compared to conventional mirrors, it is expected to provide low mechanical loss and, thus, low thermal noise. The cavity coupler was incorporated into a Fabry-Perot resonator together with a conventional high quality mirror. The finesse of this cavity was measured to be  $F = 657$ , which corresponds to a coupler reflectivity of  $R = 99.08\%$ .

© 2008 Optical Society of America

**OCIS codes:** (050.2770) Gratings; (050.6624) Subwavelength structures; (230.3990) Micro-optical devices; (230.4040) Mirrors.

---

## References and links

1. V. B. Braginsky, M. L. Gorodetsky, and S. P. Vyatchanin, "Thermodynamical fluctuations and photo-thermal shot noise in gravitational wave antennae," *Phys. Lett. A* **264**, 1–10 (1999).
2. H. J. Kimble, Y. Levin, A. B. Matsko, K. S. Thorne, and S. P. Vyatchanin, "Conversion of conventional gravitational-wave interferometers into quantum nondemolition interferometers by modifying their input and output optics," *Phys. Rev D* **65**, 022002 (2001).
3. P. Aufmuth and K. Danzmann, "Gravitational wave detectors," *New J. Phys.* **7**, 202 (2005).
4. G. M. Harry, A. M. Gretarsson, P. R. Saulson, S. E. Kittelberger, S. D. Penn, W. J. Startin, S. Rowan, M. M. Fejer, D. R. M. Crooks, G. Cagnoli, J. Hough, and N. Nakagawa, "Thermal noise in interferometric gravitational wave detectors due to dielectric optical coatings," *Class. Quantum Grav.* **19**, 897–917 (2002).
5. P. F. Cohadon, A. Heidmann, and M. Pinard, "Cooling of a Mirror by Radiation Pressure," *Phys. Rev. Lett.* **83**, 3174–3177 (1999).
6. T. Corbitt, Y. Chen, E. Innerhofer, H. Müller-Ebhardt, D. Ottaway, H. Rehbein, D. Sigg, S. Whitcomb, C. Wipf, and N. Mavalvala, "An All-Optical Trap for a Gram-Scale Mirror," *Phys. Rev. Lett.* **98**, 150802 (2007).
7. H. Müller-Ebhardt, H. Rehbein, R. Schnabel, K. Danzmann, and Y. Chen, "Entanglement of Macroscopic Test Masses and the Standard Quantum Limit in Laser Interferometry," *Phys. Rev. Lett.* **100**, 013601 (2008).
8. Y. Levin, "Internal thermal noise in the LIGO test masses: A direct approach," *Phys. Rev. D* **57**, 659–663 (1998).
9. F. Seifert, P. Kwee, M. Heurs, B. Willke, and K. Danzmann, "Laser power stabilization for second-generation gravitational wave detectors," *Opt. Lett.* **31**, 2000–2002 (2006).
10. G. Rempe, R. J. Thompson, H. J. Kimble, R. Lalezari, "Measurement of ultralow losses in an optical interferometer," *Opt. Lett.* **17**, 363–365 (1992).

11. J. Agresti, G. Castaldi, R. DeSalvo, V. Galdi, V. Pierro, and I. M. Pinto, "Optimized multilayer dielectric mirror coatings for gravitational wave interferometers," *Proc. SPIE* **6286**, (2006).
12. G. M. Harry, H. Armandula, E. Black, D. R. M. Crooks, G. Cagnoli, J. Hough, P. Murray, S. Reid, S. Rowan, P. Sneddon, M. M. Fejer, R. Route, and S. D. Penn, "Thermal noise from optical coatings in gravitational wave detectors," *Appl. Opt.* **45**, 1569–1574 (2006).
13. S. Gößler, J. Cumpston, K. McKenzie, C. M. Mow-Lowry, M. B. Gray, and D. E. McClelland, "Coating-free mirrors for high precision interferometric experiments," *Phys. Rev. A* **76**, 053810 (2007).
14. V. B. Braginsky and S. P. Vyatchanin, "Corner reflectors and quantum-non-demolition measurements in gravitational wave antennae," *Phys. Lett. A* **324**, 345–360 (2004)
15. G. A. Golubenko, A. S. Svakhin, V. A. Sychugov, and A. V. Tishchenko, "Total reflection of light from a corrugated surface of a dielectric waveguide," *Sov. J. Quantum Electron.* **15**, 886–887 (1985).
16. R. Magnusson and S. S. Wang, "New principle for optical filters," *Appl. Phys. Lett.* **61**, 1022–1024 (1992).
17. A. Sharon, D. Rosenblatt, and A. A. Friesem, "Resonant grating-waveguide structures for visible and near-infrared radiation," *J. Opt. Soc. Am. A* **14**, 2985–2993 (1997).
18. R. Nawrodt, A. Zimmer, T. Koettig, T. Clausnitzer, A. Bunkowski, E.-B. Kley, R. Schnabel, K. Danzmann, W. Vodel, A. Tünnermann, and P. Seidel, "Mechanical Q-factor measurements on a test mass with a structured surface," *New J. Phys.* **9**, 225 (2007).
19. A. Bunkowski, O. Burmeister, D. Friedrich, K. Danzmann, and R. Schnabel, "High reflectivity grating waveguide coatings for 1064 nm," *Class. Quantum Grav.* **23**, 7297–7303 (2006).
20. F. Brückner, T. Clausnitzer, O. Burmeister, D. Friedrich, E.-B. Kley, K. Danzmann, A. Tünnermann, and R. Schnabel, "Monolithic dielectric surfaces as new low-loss light-matter interfaces," *Opt. Lett.* **33**, 264–266 (2008).
21. E. Bisailon, D. Tan, B. Faraji, A. G. Kirk, L. Chrowstowski, and D. Plant, "High reflectivity air-bridge subwavelength grating reflector and Fabry-Perot cavity in AlGaAs/GaAs," *Opt. Express* **14**, 2573–2582 (2006).
22. M. G. Moharam and T. K. Gaylord, "Rigorous coupled-wave analysis of planar-grating diffraction," *J. Opt. Soc. Am.* **71**, 811–818 (1981).
23. T. Clausnitzer, T. Kämpfe, E.-B. Kley, A. Tünnermann, U. Peschel, A. V. Tishchenko, and O. Parriaux, "An intelligible explanation of highly-efficient diffraction in deep dielectric rectangular transmission gratings," *Opt. Express* **13**, 10448–10456 (2005).
24. E. Popov, M. Nevire, B. Gralak, and G. Tayeb, "Staircase approximation validity for arbitrary-shaped gratings," *J. Opt. Soc. Am. A* **19**, 33–42 (2002).
25. R. W. P. Drever, J. L. Hall, F. V. Kowalski, J. Hough, G. M. Ford, A. J. Munley, and H. Ward, "Laser Phase and Frequency Stabilization using an Optical Resonator," *Appl. Phys. B.* **31**, 97–105 (1983).
26. B. A. Usievich, V. A. Sychugov, J. KH. Nurligareev, and O. Parriaux, "Multilayer resonances sharpened by grating waveguide resonance," *Opt. Quantum Electron.* **36**, 109–117 (2004).

---

## 1. Introduction

Thermally driven motion of optical components give rise to thermal noise in high precision measurements [1], and is becoming a limiting factor for the sensitivity of interferometric experiments such as gravitational wave detectors [2, 3, 4], laser cooling of mechanical oscillators [5], optical traps for mirrors [6], and the generation of entangled test masses [7]. For dielectrically coated mirrors, the thermal noise is mainly caused by the mechanical loss of the multilayer coating stack [4, 8]. Typical coating layer materials are SiO<sub>2</sub> and Ta<sub>2</sub>O<sub>5</sub> with a major loss contribution from the latter. These two materials show very low optical absorption at the prominent laser wavelength of 1064 nm, where ultrastable solid state continuous wave laser sources exist [9], and are, therefore, frequently used in high-precision experiments. Reflectivities of multilayer coated mirrors of up to 99.9998 % have been demonstrated [10]. Thus, new concepts are required that simultaneously provide high optical quality and low mechanical loss. One approach being pursued is to design an alternative multilayer system deviating from the classical quarter wave design and containing less Ta<sub>2</sub>O<sub>5</sub> [11]. Doping of Ta<sub>2</sub>O<sub>5</sub> with TiO<sub>2</sub> has also been investigated and a reduction of the mechanical loss by a factor of 1.5 was observed [12]. Another approach is to avoid the dielectric coating at all by utilizing coating-free mirrors [13] or corner reflectors [14], which are based on total internal reflection and Brewster-angle coupling. However, in these cases thermo-refractive noise resulting from a temperature-dependent refractive index and also thermal lensing are increased due to the large optical path length inside the substrate material.

Surface relief guided-mode resonant waveguide structures [15, 16, 17] provide an alternative approach for reaching high reflectivity and simultaneously ensure low mechanical loss. Here, the coating thermal noise is reduced due to the fact that the (high-mechanical quality) substrate carries only a single, thin but corrugated high refractive index layer [18]. The focus of earlier work on waveguide grating structures was centered mainly on narrow-band filtering and switching applications [16]. However, Bunkowski *et al.* [19] theoretically investigated such a device and found parameters for a high-reflection waveguide mirror with broad spectral response. Recent theoretical research showed that even the remaining high-index layer can be avoided and that a monolithic high-reflection mirror is possible by applying an appropriate grating structure to the substrate's surface without the need for adding any other material [20]. This new approach does not imply suspended microstructures [21], which had been reported before and, therefore, overcomes the limitation to very small grating areas. Also recently, it was experimentally tested whether a periodic surface corrugation provides a significant source of mechanical loss compared to the effect of dielectric coating layers. It was found that a grating etched into the surface of a substrate had no significant effect on the substrate's quality factor, which was of the order  $10^8$  [18].

In this article, we report on the fabrication and characterization of a resonant waveguide grating based high-reflection mirror. The mirror substrate was sodalime glass and carried a single layer grating of Ta<sub>2</sub>O<sub>5</sub> (Tantala) with a thickness of 400 nm, and was used as a cavity coupler of a high-finesse standing wave cavity. From the cavity finesse we were able to deduce a reflectivity of  $(99.08 \pm 0.05)\%$  at the laser wavelength of 1064 nm. This is, to the best of our knowledge, the highest value of resonant reflection that has ever been reported. Moreover, a standing wave cavity setup has never been utilized to accurately determine a grating based resonant reflectivity before.

## 2. Resonant waveguide grating structures

Resonant waveguide grating structures employ resonant light coupling instead of multiple interference at different layer interfaces to achieve high reflectivity. They comprise a periodically nano-structured high-refractive-index layer attached to a low-refractive-index substrate. The fundamental principle of waveguide gratings is illustrated in Fig. 1 and can be understood by a simple ray picture [17]. In case of normal incidence the three following parameter inequalities (which can be derived from the well-known grating equation) have to be fulfilled to allow for resonant reflection:

$$d < \lambda \quad (\text{to permit only zeroth order in air}), \quad (1)$$

$$\lambda/n_H < d \quad (\text{first orders in high-index layer}), \quad (2)$$

$$d < \lambda/n_L \quad (\text{only zeroth order in the substrate}), \quad (3)$$

where  $d$  is the grating period,  $\lambda$  is the light's vacuum wavelength and  $n_H$  and  $n_L$  are the higher and lower refractive indices, respectively. The first diffraction orders (-1T, +1T) in the high-index layer experience total internal reflection (at the interface to the low-index substrate) and excite resonant waveguide modes. A part of the light inside the waveguide is coupled out via the grating to both, the transmitted and reflected zeroth order (0T, 0R). If the grating period  $d$ , the groove depth  $g$ , the grating fill factor  $f$  (ratio between ridge width  $r$  and grating period  $d$ ), and the high-index layer thickness  $s$  with respect to the refractive index values of the involved materials are designed properly, all transmitted light can be prompted to interfere destructively, corresponding to a theoretical 100 % reflectance.

With decreased coupling efficiency to the waveguide modes the structure behaves more resonant leading to a higher finesse of the single peak reflection spectrum [17]. That property makes

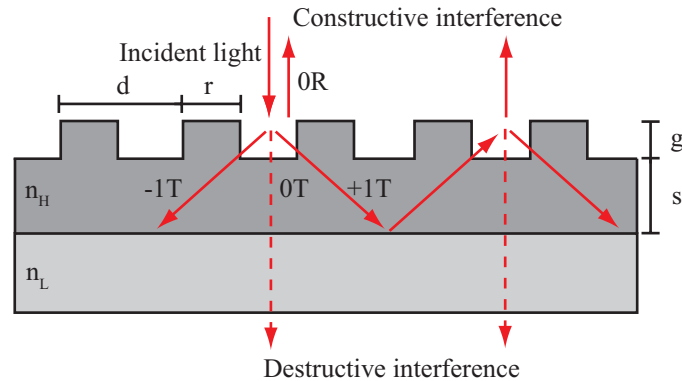


Fig. 1. Fundamental principle of resonant waveguide gratings in a simplified ray picture.

such devices suitable for narrow-band filtering. However, for applications as mentioned above, a broadband resonance is desired, since small deviations from the device's design parameters would dramatically decrease the normal incidence reflectivity for the central wavelength. Additionally, an electric field enhancement inside a high-finesse waveguide might be a problem for high-power laser interferometry due to laser induced damage. The spectral response can be significantly broadened by increasing the coupling efficiency via a theoretical parameter design as it is performed in [19].

Today's gravitational wave detectors use fused silica as the test mass material ( $n_L \approx 1.5$ ) and Nd:YAG lasers as ultrastable light sources with a central wavelength of  $\lambda = 1064$  nm [3]. The most common high-index material for this wavelength region is tantala with a refractive index of  $n_H \approx 2.1$  [4]. In the following we restrict ourselves to this material combination and wavelength. According to Ineqs. (1) - (3), the grating period is restricted by  $512 \text{ nm} < d < 710 \text{ nm}$ . For systematic design considerations in terms of broad resonance behavior, we refer to [19], wherein a Rigorous-Coupled-Wave Analysis (RCWA) [22] was used to find appropriate grating parameters with high reflectivity as well as convenient fabrication tolerances. These simulations included three free parameters besides the grating period  $d$ , namely the groove depth  $g$ , the waveguide thickness  $s$  and the grating fill factor  $f$ . As a result, assuming TM-polarized light (electric field oscillating perpendicular to the grating ridges) and a rectangular grating profile, for the purpose of a broadband reflection peak, large values for the grating period close to 700 nm are favorable. Moreover, the simulations showed that high TM-reflectivity can even be found for zero waveguide layer thickness ( $s = 0$  nm), if the groove depth and the grating fill factor are about  $g \approx 400$  nm and  $f \approx 0.5$ , respectively. As the overall thickness of the high-index coating material is the crucial factor for coating thermal noise, the reduction of the residual waveguide layer down to zero would be highly beneficial [18]. The effective tantala layer thickness in this case ( $g = 400$  nm,  $f = 0.5$ ) is only about  $0.2 \mu\text{m}$  in contrast to a conventional mirror, typically comprising an 18 double-layer dielectric stack with an overall tantala thickness of about  $3 \mu\text{m}$ . This suggests a significant thermal noise reduction.

Please note that for vanishing waveguide layer thickness the simplified ray picture breaks down. The diffraction orders that are involved in the coupling process rather need to be considered as corresponding to discrete grating modes propagating through the binary grating region. For a more detailed explanation we refer the reader to [23]. However, the simulations are based on a RCWA which is still valid for  $s = 0$  nm.

### 3. Fabrication process

For the fabrication of the desired waveguide grating, a sodalime glass substrate with an index of refraction of  $n_L = 1.515$  was first coated with a 400 nm tantala layer with an index of refraction of  $n_H = 2.105$  by means of Plasma-Ion-Assisted Deposition (PIAD). With regard to the desired groove depth, sodalime glass was chosen as the substrate material instead of fused silica since it remains nearly unaffected while the tantala etching process. The grating with a period of  $d = 690$  nm was defined by the use of electron beam lithography for an area of  $(75 \text{ mm})^2$ , aiming at a grating fill factor of  $f = 0.515$ . The final Inductively-Coupled-Plasma (ICP) etching step was adjusted to match the desired grating groove depth of  $g = 400$  nm, which corresponds to a zero waveguide layer thickness ( $s = 0$  nm). Figure 2 depicts a top view scanning electron microscope (SEM) image of the grating used in the experiment (left hand side) and a cross-sectional view of the resulting grating profile of a grating from the same fabrication process, but different fill factor (right hand side), revealing that the actual groove depth was just slightly deviating from the target value.

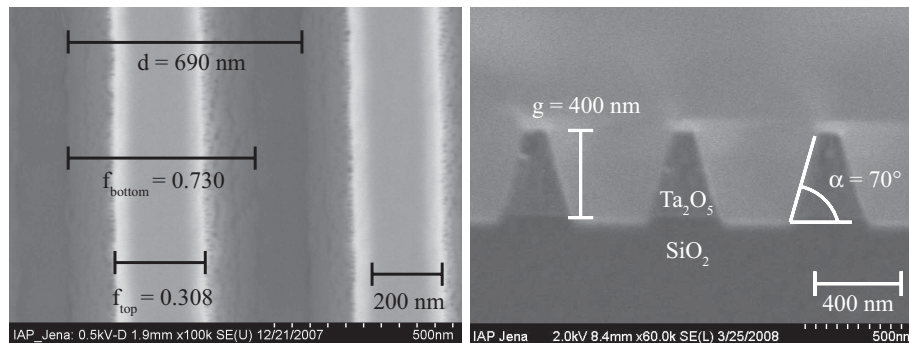


Fig. 2. Left hand side: Top view of the fabricated resonant waveguide grating with trapezoidal grating profile. The accurate values for the fill factors arose from the spectral fit in Fig. 3. Right hand side: Cross-sectional view of a related grating with the same groove depth but different fill factor.

However, the tantala grating ridges were found to exhibit a trapezoidal shape instead of a rectangular one which had been assumed for the design considerations in [19]. Most likely the ICP etching process was affected by a crystal formation within the tantala layer during its deposition. Subsequent rigorous simulation using a staircase approximation [24] showed that such a trapezoidal profile is still capable of high reflectivity while the bandwidth remains substantially unaffected.

From the left hand side of Fig. 2, we realized an effective fill factor of 0.52 instead of 0.515 which would give a maximum in reflectivity. This leads to a stronger dependence of the reflectivity to variations of the grating parameters over the grating area that occur in the fabrication process.

### 4. Experimental characterization

The spectral transmittance under near normal incidence ( $0 \pm 1$ ) $^\circ$  was measured using a fiber-based white-light source and a spectrum analyzer with a resolution of 50 pm. The measured data is shown in Fig. 3 (black curve) and reveals a minimum transmittance of 0.19 % at a wavelength of  $\lambda = 1065.6$  nm and a transmittance of 0.8 % at the central wavelength  $\lambda = 1064$  nm. The kink near  $\lambda = 1045$  nm is related to the incipient transmission of the first diffracted orders into the substrate material since the condition for total internal reflection is no longer fulfilled at

this wavelength, see Ineq. (3). The spectral bandwidth of the resonant device shows a broad transmission of  $\leq 10\%$  over a wavelength range of 12 nm. Assuming a grating period of  $d = 690$  nm, a groove depth of  $g = 400$  nm ( $s = 0$  nm) and a side wall angle of  $\alpha = 70^\circ$ , which can be estimated with the cross-sectional SEM image on the right hand side of Fig. 2, the best fitted spectral response was achieved with a top fill factor of  $f_{\text{top}} = 0.308$ , see red curve in Fig. 3.

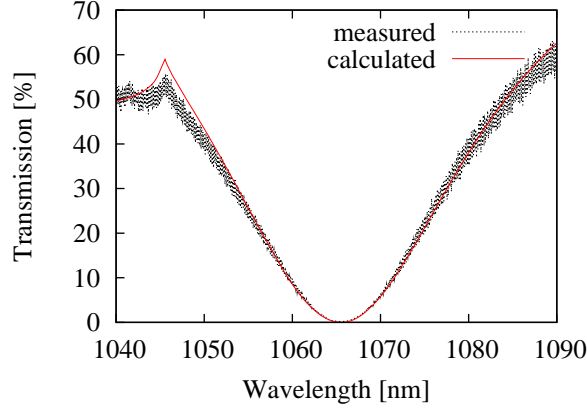


Fig. 3. Spectral zeroth order transmittance of the resonant grating-based cavity coupler under normal incidence and for TM-polarization.

Setting up a linear Fabry-Perot resonator with the waveguide grating as a coupling mirror enabled us to exactly adjust the angle of incidence to be zero degree and was used to determine the reflectivity at a wavelength of 1064 nm. The experimental setup is sketched in Fig. 4(a). The light source was a Nd:YAG laser with a wavelength of 1064 nm. The light was spatially filtered by a ring modecleaner (MC) which was stabilized via the Pound-Drever-Hall (PDH) control scheme [25]. Therefore, a phase modulation at 12.18 MHz was used that was imprinted on the light by means of an electro-optical modulator (EOM). The linear Fabry-Perot resonator was set up with the waveguide grating and a superpolished, high reflectivity end mirror which has a measured transmission of  $T_{\text{end}} = (300 \pm 30)$  ppm. The length of the cavity  $L = (0.495 \pm 0.001)$  m defines its free-spectral range  $\text{FSR} = c/2L$ . The linewidth (full width at half maximum)  $\Delta\nu$  was measured in order to determine the Finesse  $F = \text{FSR}/\Delta\nu$  and subsequently the reflectivity of the grating device.

In order to obtain the cavity linewidth we calibrated the cavity detuning by using the PDH phase modulation signals as frequency markers around an airy peak, see Fig. 4(b). For this purpose, the residual sideband fields at 12.18 MHz transmitted through the modecleaner were used. The linewidth was averaged over twenty measurements, which resulted in  $\Delta\nu = (461 \pm 19)$  kHz, where we took a 4% error into account for the linewidth and a 1% uncertainty for the frequency markers. Hence, the Finesse was  $F = 657 \pm 27$ . Since the product of the amplitude reflectivities  $\rho_1$  and  $\rho_2$  of the end mirror and waveguide grating, respectively, is connected to the Finesse by

$$\rho_1\rho_2 = 2 - \cos\left(\frac{\pi}{F}\right) - \sqrt{\left(\cos\left(\frac{\pi}{F}\right) - 2\right)^2 - 1}, \quad (4)$$

we find the waveguide grating power reflectivity to be  $\rho_2^2 = (99.08 \pm 0.05)\%$ . Here, any resonant reflection phase shift [26] can be neglected since the light source is a single frequency laser. Though this value is a record for measured resonant reflection, it still does not compete

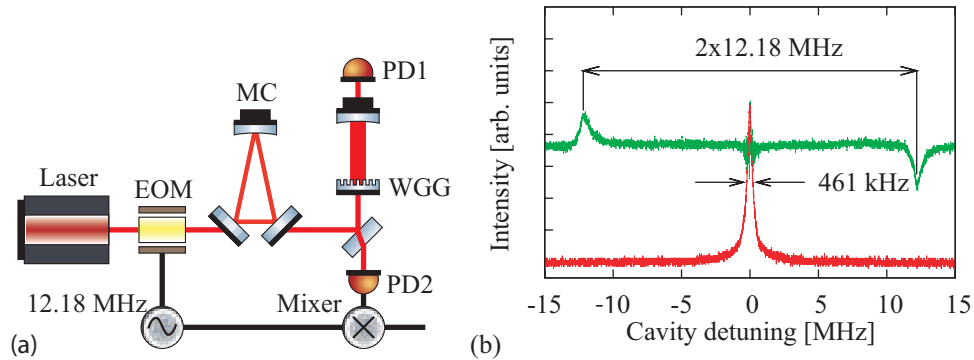


Fig. 4. (a) Experimental setup for the characterization of the waveguide grating (WGG) as a cavity coupling mirror. Electro-optical-modulator (EOM), modecleaner (MC), photodiode (PD). (b) Scan over one airy peak (red) of linewidth 461 kHz measured in transmission (PD1). The cavity detuning was calibrated via the demodulated signal (green) in reflection of the cavity (PD2).

with conventional multilayer mirrors when only regarding optical loss [10]. We would like to point out that the spectral measurement as well as the cavity setup were optimized to lowest transmission by adjusting the beam position on the grating. The reflectivity over the entire grating area was found to be higher than 96% with a spatial resolution given by the beam radius of  $\approx 130\ \mu\text{m}$ . These variations can be explained by a deviation of the effective fill factor in the range between 0.52 and 0.525. Assuming a fill factor of 0.515, the same deviation would lead to a reflectivity higher than 99.6% over the whole area.

## 5. Conclusion

For the purpose of pushing highly reflective optical components towards a low thermal noise regime, we demonstrated a coupler for a standing wave cavity based on a guided-mode resonant grating device. By periodically structuring a 400 nm tantala layer on top of a sodalime glass substrate we achieved a reflectivity of 99.08% for a wavelength of 1064 nm and TM-polarized light. By utilizing strong resonant light coupling a broad spectral bandwidth with a transmission of  $\leq 10\%$  over a wavelength range of 12 nm could be obtained. Simultaneously, low coating thermal noise can be expected due to a vastly decreased effective tantala layer of only about  $0.2\ \mu\text{m}$  compared to conventional mirrors with an overall tantala thickness of about  $3\ \mu\text{m}$ . For future work we plan to characterize the performance of an all grating-based standing wave cavity with prospects for implementation in all-reflective interferometric setups for future gravitational wave detectors. Especially, the thermal noise level of this cavity compared to conventional setups will be of great interest.

## Acknowledgments

This work was supported by the Deutsche Forschungsgemeinschaft within the Sonderforschungsbereich TR7.